

# Viscous Incompressible Flows by the Velocity-Vorticity Navier-Stokes Equations

Alfredo Nicolás<sup>1</sup> and Blanca Bermúdez<sup>2</sup>

**Abstract:** 2D viscous incompressible flows are presented from the unsteady Navier-Stokes equations in its velocity-vorticity formulation. The results are obtained using a simple numerical procedure based on a fixed point iterative process to solve the nonlinear elliptic system that results once a second order time discretization is performed. Flows on the un-regularized unit driven cavity problem are reported up to Reynolds numbers  $Re=4000$  to compare them with those reported by other authors, mainly solving the steady problem, and supposed to be correct. Moreover, results are reported for  $Re = 1000, 4000, 5000,$  and  $10000$  to see how their flows look like close from its departure  $t = 0$ .

## 1 Introduction

The main goal of this paper is to present 2D viscous incompressible flows from the unsteady Navier-Stokes equations in its velocity-vorticity formulation. These flows are obtained by applying a numerical procedure based mainly on a fixed point iterative process to solve the nonlinear elliptic system that results once a convenient second order time discretization is made. The iterative process leads to the solution of uncoupled, well-conditioned, symmetric linear elliptic problems for which very efficient solvers exist either by finite differences or finite elements as far as rectangular domains are considered.

Flows on the un-regularized unit driven cavity problem are reported to validate the numerical procedure up to Reynolds numbers  $Re = 4000$

with those in Schreiber and Keller (1983) from the steady problem as well as those in Nicolás and Bermúdez (2004) from the unsteady problem; both works in terms of the stream function-vorticity formulation. Beyond this validation, results are reported for  $Re = 1000, 4000, 5000,$  and  $10000$  to see how their flows look like close from its departure  $t = 0$ . These either transient or *time-dependent* flows show the ability of the numerical procedure to start directly from the initial condition at  $t = 0$  and not necessarily from a smaller Reynolds number previously calculated.

Taking into account that solving the unsteady problem a steady state is supposed to exist for  $Re \leq 7500$ , some facts are addressed next on the steady state results reported here up to  $Re = 4000$ , up to  $Re = 5000$  in Nicolás and Bermúdez (2004).

1) As can be seen in several other works, say Schreiber and Keller (1982) solving the steady problem in the stream function-vorticity variables formulation, Ghia et al. (1982) and Goyon (1996) solving the unsteady one with the same formulation, like in Nicolás and Bermúdez (2004), in the steady state, agreeing with the solution of the steady problem, the vorticity is concentrated close to the solid parts of the boundary, being not zero there by boundary layer effects associated with viscosity, Landau and Lifshitz (1989). 2) In connection with this, an interesting aspect is to see what happens with the vorticity before the steady state is reached; that is, what happens in the transient stage, an aspect not usually considered so far due to the fact that most numerical schemes cannot compute the flow directly from the initial condition  $t = 0$  but from the flow of a smaller Reynolds number previously computed. Interesting as well is to see what happens with the corresponding vorticity for a time-dependent flow, say  $Re = 10000$ . As the results show, close from

<sup>1</sup>Depto. Matemáticas, 3er. Piso Ed. Diego Bricio, UAM-Iztapalapa, 09340 México D.F. México, e-mail: anc@xanum.uam.mx

<sup>2</sup>Facultad de C. de la Computación, BUAP, Pue., México, e-mail: bbj@solarium.cs.buap.mx *correspondence to:* Alfredo Nicolás

its departure  $t = 0$ , the vorticity being spread all over the cavity for  $Re = 10000$  tends to concentrate close to the solid parts of the boundary as  $Re$  decreases since the fixed final time is closer to the time where the asymptotic steady state occurs, this time being smaller as  $Re$  is smaller. Unlike the situation showed here, the vorticity of the results close from  $t = 0$  for  $Re \geq 10000$  shown in Nicolás and Bermúdez (2004) is spread all over the cavity since they are supposed to be time-dependent flows.

Based on the experience of the authors with the 2D solution of the driven cavity problem with the *three* formulations of the Navier-Stokes equations: primitive variables, stream function-vorticity, and velocity-vorticity we would like to point out that is easier to get the results with the contour values given by Schreiber and Keller (1982) than with those by Ghia et al. (1982), meaning by this that the results can be obtained with a coarser mesh; moreover, it is more difficult to get the vorticity with the contour values in Ghia et al. (1982): if the numerical method works a finer mesh is required. That this is not a trivial task to deal with is reflected in the fact that several published works report only the streamlines.

In Nicolás and Bermúdez (2004) it was possible to obtain steady state flows up to  $Re = 5000$  as well as to obtain time-dependent flows close from its departure  $t = 0$  for higher Reynolds numbers than the one reported here; moreover, it was also possible to obtain various long time computations for  $Re=10000$  to illustrate its evolution as time-dependent flow. On the other hand, the meshes needed for them, even for the steady state results, are coarser than those used here. Then, because not all the analogous results are obtained, considering also that the meshes are coarser, it can be concluded that with the velocity-vorticity formulation is more difficult to solve these flows, at least with a numerical procedure very similar to the one applied in the stream function-vorticity formulation, mainly using a fixed point iterative process to solve the elliptic non-linear system that results after time discretization, and taking likely other aspects: no up-winding ingredient is used, the meshes follow also the size dictated by

the thickness of the boundary layer (of order of  $Re^{-1/2}$ ), and no refining of the mesh is used near the boundary.

Some works on velocity-vorticity formulation are mentioned next. Fusegi and Farouck (1986) use a control-volume finite difference approach to discretize the problem and then a direct solution procedure (along a grid line) to solve the algebraic system via a block tridiagonal matrix algorithm. They present isothermal results for the driven cavity problem also, and heat transfer results for natural and mixed convection. Lo et al. (2005) present 3D results for the driven cavity problem up to  $Re \leq 2000$  using finite differences combined with an ADI procedure for the parabolic velocity Poisson equations and the continuity equation to solve the resultant algebraic system by a diagonally dominant tridiagonal matrix algorithm. In Tsai et al. (2002) a meshless BEM method is developed to solve 3D Stokes flows with this formulation. Surprisingly, the iterative process used is very close to ours, the only difference is that ours is a truly fixed point one, with a different time discretization. Actually, they claim that their method can be extended to the 3D velocity-vorticity Navier-Stokes equations. Grimaldi et al. (2006) through a Parallel multi-block method report results for 2D and 3D for the driven cavity problem; for 2D, the horizontal and vertical velocity profiles at the center of the cavity are shown for  $Re = 1000$ . Chantasiriwan (2006) reports driven cavity results for the low Reynolds numbers  $Re = 0$ , which turns out to be a Stokes flow because of its infinity viscosity, and  $Re = 100$  using a Multiquadric collocation method. Mai-Duy and Tran-Cong (2004) with the primitive variables formulation, report also the driven cavity flow for  $Re = 100$  using the one for  $Re = 0$  as the initial interface solution in their domain decomposition technique.

This paper is organized as follows: In Section 2 the problem is formulated, in Section 3 the numerical method is described, the numerical experiments appear in Section 4 and in Section 5 some conclusions are made. On Section 4 we proceed as follows: 1) Asymptotic steady results for  $400 \leq Re \leq 4000$ , from the unsteady prob-

lem, are presented as a validation matter of the numerical method; they are compared with those in Schreiber and Keller (1983) obtained by solving the steady problem. To reinforce this validation, for  $Re = 1000$  a kind of mesh independence is showed through some velocity profiles, from which the optimal mesh that works for this case is chosen and it is taken as a guide to choose the appropriate meshes for the other Reynolds numbers. 2) Results for  $Re = 1000, 4000, 5000,$  and  $10000$  are shown to see how their flows look like close from its departure  $t = 0$ .

## 2 The Navier-Stokes equations in velocity-vorticity form

Let  $\Omega \subset R^N (N = 2, 3)$  be the region of the unsteady flow of a viscous incompressible fluid, and  $\Gamma$  its boundary. This kind of time dependent flow is governed by the non-dimensional equations, in  $\Omega \times (0, T), T > 0$ ,

$$\mathbf{u}_t - \frac{1}{Re} \nabla^2 \mathbf{u} + \nabla p + (\mathbf{u} \cdot \nabla) \mathbf{u} = \mathbf{f} \quad (1a)$$

$$\nabla \cdot \mathbf{u} = 0 \quad (1b)$$

known as the Navier-Stokes equations in primitive variables  $\mathbf{u}$ , velocity, and  $p$ , pressure. The parameter  $Re$  is the Reynolds number and  $\mathbf{f}$  is a given concentration of external forces.

To get, in principle, a unique solution in a bounded region  $\Omega$ , initial and boundary conditions must be supplied, say  $\mathbf{u}(\mathbf{x}, 0) = \mathbf{u}_0(\mathbf{x})$  in  $\Omega$  and for instance  $\mathbf{u} = \mathbf{g}$  on  $\Gamma$ , respectively. As is well known, unlike in 3D, in 2D a unique solution exists, weakly speaking, for problem (1a – 1b), with initial and boundary conditions, for all time  $t \geq 0$  regardless of the Reynolds number.

By taking the curl in both sides of equation (1a) one obtains the non-dimensional form of the vorticity  $\omega$  transport equation in  $\Omega \times (0, T)$

$$\omega_t - \frac{1}{Re} \nabla^2 \omega + \mathbf{u} \cdot \nabla \omega = \omega \cdot \nabla \mathbf{u} + \mathbf{f} \quad (2)$$

where the vorticity vector  $\omega$  is defined by

$$\omega = \nabla \times \mathbf{u} \quad (3)$$

and the new  $\mathbf{f}$  is the curl of the old one.

Taking the curl of equation (3) and using the incompressibility constraint (1b), from the identity  $\nabla \times \nabla \times \mathbf{a} = -\nabla^2 \mathbf{a} + \nabla(\nabla \cdot \mathbf{a})$ , the following velocity Poisson equation is obtained

$$\nabla^2 \mathbf{u} = -\nabla \times \omega \quad (4)$$

Equations (2) and (4) are the velocity-vorticity form of the Navier-Stokes equations, with three equations for the velocity vector  $\mathbf{u} = (u_1, u_2, u_3)$  and three equations for the vorticity vector  $\omega = (\omega_1, \omega_2, \omega_3)$  in Cartesian co-ordinates.

Equations (2) and (4), like those in (1a – b), can handle in general 3D flows; however, in this work numerical results are presented for 2D flows only. Some details of this case follows.

It can be easily verified that the vorticity, scalar,  $\omega$  transport equation in  $\Omega \times (0, T), \Omega \subset R^2$ , is given by

$$\omega_t - \frac{1}{Re} \nabla^2 \omega + \mathbf{u} \cdot \nabla \omega = f \quad (5)$$

where, from the 2D restriction in (3),

$$\omega = \frac{\partial u_2}{\partial x} - \frac{\partial u_1}{\partial y} \quad (6)$$

and, from (4), the two Poisson equations for the velocity components are expressed as

$$\nabla^2 u_1 = -\frac{\partial \omega}{\partial y} \quad (7a)$$

$$\nabla^2 u_2 = \frac{\partial \omega}{\partial x} \quad (7b)$$

Then, the vector system (2) and (4) is reduced to a scalar system of three equations in 2D: one from the form (2) for  $\omega$  given by (5) and two from (4) for  $u_1$  and  $u_2$  given by (7), related each other through (6) from which the boundary condition for  $\omega$  in (5) should be obtained from the one of  $\mathbf{u} = (u_1, u_2)$ .

It must be noted that the 2D scalar system (5)-(7) has the advantage to the so called stream function-vorticity variables formulation since the velocity  $\mathbf{u}$  is computed explicitly. Actually, the stream function  $\psi$  is trivially computed solving a Poisson equation with  $\omega$  computed in (5) as the right hand side; that is

$$\nabla^2 \psi = -\omega \quad (8)$$

obtained from the definition of  $\omega$  given by (6) and the definition of  $\psi$  in terms of  $u_1$  and  $u_2$ :

$$u_1 = \frac{\partial \psi}{\partial y}, \quad u_2 = -\frac{\partial \psi}{\partial x} \quad (9)$$

which follows from (1b); the equation must be supplemented by the  $\psi$  boundary condition implied by the one from  $\mathbf{u}$ . Equations (9) and (5) give the so called stream function-vorticity formulation of the Navier-Stokes equations in 2D.

Another approach to solve (7) is to embedding it into a time-depending problem, in  $\Omega \times (0, T)$ ,

$$\frac{\partial u_1}{\partial t} - \nabla^2 u_1 = \frac{\partial \omega}{\partial y} \quad (10a)$$

$$\frac{\partial u_2}{\partial t} - \nabla^2 u_2 = -\frac{\partial \omega}{\partial x} \quad (10b)$$

and look for the steady state of the flow, if any, as  $t$  approaches to  $+\infty$  (large  $t$  in practice).

Following Fusegi and Farouck (1986), some aspects on the velocity-vorticity formulation must be pointed out. Although continuity, that is, incompressibility condition (1b), was assumed to be satisfied for the derivation of equations (4), and hence for equations (7), there is not guaranty it must be hold for the difference equations.

Let

$$D = \frac{\partial u_1}{\partial x} + \frac{\partial u_2}{\partial y} = 0 \quad (11)$$

By differentiating the equations appearing in (7) with respect to  $x$  and  $y$  respectively, and adding the resulting equations, it follows that

$$\nabla^2 D = 0 \quad (12)$$

Then, by the maximum principle, if  $|D| = 0$  on the boundary it follows that continuity,  $D = 0$ , holds in the entire domain of the flow. As can be seen next, the numerical experiments are given for the so called un-regularized driven cavity problem; then continuity is satisfied.

The numerical experiments of this work are concerned with the well known un-regularized driven cavity problem which implies re-circulation phenomena because of its velocity boundary condition. Then, equations (1) are set in the domain

$\Omega = (0, 1) \times (0, 1)$  and the boundary condition, in terms of  $\mathbf{u}$  is defined by  $\mathbf{u} = (1, 0)$  at the moving boundary (the top one) and  $\mathbf{u} = (0, 0)$  elsewhere. So, the components of these relations give the boundary conditions for equations (7) to get  $u_1$  and  $u_2$  whereas the  $\omega$  boundary condition to solve the vorticity equation (5) follows from (6) and are given by

$$\begin{cases} u_1 = 0, \quad u_2 = 0, \quad \omega = \frac{\partial u_2}{\partial x} & \text{on } \Gamma_{x=0} \\ u_1 = 0, \quad u_2 = 0, \quad \omega = \frac{\partial u_2}{\partial x} & \text{on } \Gamma_{x=1} \\ u_1 = 0, \quad u_2 = 0, \quad \omega = -\frac{\partial u_1}{\partial y} & \text{on } \Gamma_{y=0} \\ u_1 = 1, \quad u_2 = 0, \quad \omega = -\frac{\partial u_1}{\partial y} & \text{on } \Gamma_{y=1}. \end{cases} \quad (13)$$

In addition,  $\omega(\mathbf{x}, 0) = \omega_0(\mathbf{x})$  denotes the initial condition for the vorticity which, by (3), has to satisfy  $\omega_0 = \frac{\partial u_{02}}{\partial x} - \frac{\partial u_{01}}{\partial y}$  if  $\mathbf{u}_0 = (u_{01}, u_{02})$  is the initial velocity.

### 3 Numerical method

For the time derivative appearing in the vorticity equation (5) the following well known second-order approximation is used

$$\omega_t(\mathbf{x}, (n+1)\Delta t) = \frac{3\omega^{n+1} - 4\omega^n + \omega^{n-1}}{2\Delta t}, \quad (14)$$

where  $\mathbf{x} \in \Omega$ ,  $n \geq 1$ , and  $\Delta t$  denotes the time step and  $\omega^r \equiv \omega(\mathbf{x}, r\Delta t)$  for  $\omega$  smooth enough.

The implicit time-discretization system (5) and (7) reads, in  $\Omega$ ,

$$\begin{cases} \nabla^2 u_1^{n+1} = -\frac{\partial \omega^{n+1}}{\partial y} \\ \nabla^2 u_2^{n+1} = \frac{\partial \omega^{n+1}}{\partial x} \\ \alpha \omega^{n+1} - \nu \nabla^2 \omega^{n+1} + \mathbf{u}^{n+1} \cdot \nabla \omega^{n+1} = f_\omega \end{cases}, \quad (15)$$

where  $\alpha = \frac{3}{2\Delta t}$ ,  $f_\omega = \frac{4\omega^n - \omega^{n-1}}{2\Delta t}$ , and  $1/Re$  has been replaced by the kinematic viscosity  $\nu$ .

Then, at each time step the following nonlinear system of elliptic equations must be solved in  $\Omega$

$$\begin{cases} \nabla^2 u_1 = -\frac{\partial \omega}{\partial y} \\ \nabla^2 u_2 = \frac{\partial \omega}{\partial x} \\ \mathbf{u} = \mathbf{u}_{bc} & \text{on } \Gamma \\ \alpha \omega - \nu \nabla^2 \omega + \mathbf{u} \cdot \nabla \omega = f \\ \omega = \omega_{bc} & \text{on } \Gamma, \end{cases} \quad (16)$$

where  $\mathbf{u}_{bc}$  and  $\omega_{bc}$  denote the boundary condition for  $\mathbf{u}$  and  $\omega$  respectively, given in (13). To obtain  $u_1^1$ ,  $u_2^1$ , and  $\omega^1$  in (15), an Euler first-order approximation is applied for the time derivative through a subsequence with a smaller time step to keep up with second-order accuracy. A system of the form (16) is also obtained. If equations (10) were solved instead of equations (7), after approximating the time-derivatives by (14), a system like (16) would be also obtained.

Taking into account that the elliptic system (16), in addition to be nonlinear, is of non-potential (or transport) type, a fixed point iterative process is used to solve it. This process is similar to one applied to thermal problems, in connection with mixed convection in primitive variables, Bermúdez and Nicolás (1999), and in stream function-vorticity variables, Nicolás and Bermúdez (2005); and as already mentioned in the Introduction, in connection with isothermal problems in stream function-vorticity variables too, Nicolás and Bermúdez (2004).

Denoting

$$R(\omega) \equiv \alpha\omega - \nu\nabla^2\omega + \mathbf{u} \cdot \nabla\omega - f \text{ in } \Omega \quad (17)$$

then, system (16) is equivalent to, in  $\Omega$ ,

$$\begin{cases} \nabla^2 u_1 = -\frac{\partial\omega}{\partial y} \\ \nabla^2 u_2 = \frac{\partial\omega}{\partial x} \\ \mathbf{u} = \mathbf{u}_{bc} & \text{on } \Gamma \\ R(\omega) = 0, \omega = \omega_{bc} & \text{on } \Gamma \end{cases} \quad (18)$$

Then, (18) is solved, at time level  $(n+1)$ , by the fixed point iterative process

With  $\omega^0 = \omega^n$  given, until convergence on  $\omega$  solve

$$\begin{cases} \nabla^2 u_1^{m+1} = -\frac{\partial\omega^m}{\partial y} \\ \nabla^2 u_2^{m+1} = \frac{\partial\omega^m}{\partial x} \\ \mathbf{u}^{m+1} = \mathbf{u}_{bc} & \text{on } \Gamma, \\ \omega^{m+1} = \omega^m - \rho(\alpha I - \nu\nabla^2)^{-1}R(\omega^m) \\ \omega^{m+1} = \omega_{bc} & \text{on } \Gamma; \rho > 0, \end{cases} \quad (19)$$

then take  $(u_1^{n+1}, u_2^{n+1}, \omega^{n+1}) = (u_1^{m+1}, u_2^{m+1}, \omega^{m+1})$ .

Finally, system (19) is equivalent to, in  $\Omega$ ,

$$\begin{cases} \nabla^2 u_1^{m+1} = -\frac{\partial\omega^m}{\partial y} \\ \nabla^2 u_2^{m+1} = \frac{\partial\omega^m}{\partial x} \\ \mathbf{u}_{bc}^{m+1} = \mathbf{u}_{bc} & \text{on } \Gamma, \\ (\alpha I - \nu\nabla^2)\omega^{m+1} = (\alpha I - \nu\nabla^2)\omega^m - \rho R(\omega^m) \\ \omega^{m+1} = \omega_{bc} & \text{on } \Gamma. \end{cases} \quad (20)$$

It turns out that at each iteration *three* uncoupled elliptic linear problems associated with the operators  $\nabla^2$  and  $\alpha I - \nu\nabla^2$  have to be solved; it should be noted that the non-symmetric part for  $\omega$  has been taken into the right hand side thanks to the iterative process. Therefore, the solution of the original system, at each iteration of each time level, leads to the solution of standard symmetric linear elliptic problems.

It is well known that for the space discretization of elliptic problems like those in (20), either finite differences or finite elements may be used, as far as rectangular domains are concerned; it is also known that in either case very efficient solvers exist. In the finite element case, variational formulations have to be chosen and then restrict them to the finite dimensional finite elements spaces, for instance like those in Gunzburger (1989), Dean et al. (1991), and Glowinski (2003). For the specific results in the following Section, the second order approximation of the Fishpack solver in rectangular domains, Adams et al. (1980), has been used, where the corresponding algebraic linear systems are solved through an efficient cyclic reduction iterative method, Sweet (1977). Then, such second order approximation in space combined with the second order approximation in time (14), imply that the whole approximate problem is based on second order discretizations.

As indicated at the beginning of the next Section, contrary to what it was thought not all the results could be obtained with second order discretizations; then, a fourth order one was required for some of them. The fourth order discretization is accomplished with the fourth order option of Fishpack to approximate the elliptic problems and with the one in Burden and Faires (1985) to approximate the first derivatives.

#### 4 Numerical experiments

First of all, it is pointed out that the results that follow for small Reynolds numbers,  $Re=400$  and  $1000$ , were obtained with  $4^{th}$  order approximations, for the higher ones  $Re=4000$  and  $5000$  with  $2^{th}$  order, and for the highest  $Re = 10000$  with  $4^{th}$  order. Because the fluid motion is lower for smaller Reynolds numbers, in the first two sets the opposite might be expected.

The initial condition for velocity and vorticity are given by  $\mathbf{u}(\mathbf{x},0) = (0,0)$  and  $\omega(\mathbf{x},0) = 0$ . The parameter  $\rho$  in the iterative process is chosen as  $\rho = 0.7$  with stopping absolute criterion given by  $10^{-7}$ . The Reynolds number  $Re$  considered in the numerical experiments lies in the range  $400 \leq Re \leq 10000$ . The results are reported through the streamlines of the stream function (right part of the pictures) and the iso-vorticity contours (left part); the iso-contours values, are those given by Schreiber and Keller (1983). The discretization parameters, time step  $\Delta t$  and mesh size  $h$ , will be specified in each case under study.

All the results shown correspond to either steady state flows obtained from the unsteady problem, which are the converged asymptotic steady state obtained as time  $t$  approaches to  $+\infty$  (large time in practice), or flows close from its departure  $t = 0$ .

1). The results for  $Re = 400, 1000, 4000$  correspond to the asymptotic steady state and they are compared with those in Schreiber and Keller (1983) by solving the steady problem.

Figure 1 shows the profile of  $u_2$  at  $y = 0.5$  whereas Figure 2 the one of  $u_1$  at  $x = 0.5$  for  $Re = 400$ , with  $h = 1/100$ , and  $Re = 1000$ , with  $h = 1/140$ ; in both cases  $\Delta t = 0.01$ . It is observed that there is good agreement with those in Schreiber and Keller (1983). In Figure 3 and Figure 4 through the analogous profiles as before a kind of mesh independence is shown for  $Re = 1000$  on three meshes:  $h = 1/100$ ,  $h = 1/140$ , and  $h = 1/400$ . As can be observed the results are almost indistinguishable for the latter two. Then,  $h = 1/140$  is chosen as the good one, and we take this size as a guide for  $Re = 400, 4000, 5000$ , and  $10000$ . We mention in passing that the profiles for  $Re = 400$  and  $1000$  agree also with those in Shu et al.

(2005) from the stream function-vorticity formulation, taking into consideration that the profiles for the horizontal velocity  $u_1$  show a kind of rotation since in their stream function-vorticity formulation the stream function equation is not minus the vorticity as it must be in the general case.

To reinforce the mesh size choice, the streamlines and iso-vorticity contours for  $Re = 400, 1000$ , and  $4000$  are compared with those in Schreiber and Keller (1983). To this end: Figure 5 shows the contours for  $Re = 400$  with  $h = 1/100$ , Figure 6 for  $Re = 1000$  with  $h = 1/140$ ; both with  $\Delta t = 0.01$ ; and Figure 7 shows the ones for  $Re = 4000$  with  $h = 1/600$  and  $\Delta t = 0.002$ . In all cases a perfect agreement is obtained; the results for  $Re = 400$  and  $1000$ , with different meshes, coincide also with those in Nicolás and Bermúdez (2004).

2). A set of results follows for  $Re = 1000, 4000, 5000$ , and  $10000$  to show how the flows look like close from its departure  $t = 0$ , all of them computed at the specific final time  $T = 25$ .

Figure 8 shows such flow for  $Re = 4000$  and Figure 9 the one for  $Re = 5000$ ; both with  $h = 1/600$  and  $\Delta t = 0.002$ . Finally, Figure 10 shows the flow for  $Re = 10000$  with  $h = 1/512$  and  $\Delta t = 0.0002$ . It is worth noticing that the result for  $Re = 4000$  in Figure 8, concerning the vorticity contours, looks very similar to the one in Mai-Duy et al. (2007) for the close  $Re = 3200$  where a different method is used on the stream function-vorticity formulation.

The result for  $Re = 1000$ , at  $T = 25$ , is not presented because it looks like the same shown in Figure 6, which was obtained at a bigger final time  $T$  to make sure that the steady state was already reached. However, comparing this result at  $T = 25$  with the others we have: as long as  $Re$  decreases from  $10000$  to  $1000$ , at  $T = 25$  fixed, the vorticity, with contour values different from zero (given this way by Schreiber and Keller (1983)) concentrates close to the solid parts of the boundary, because of boundary layer effects associated with viscosity, as already mentioned in the Introduction, but before the steady state it is still concentrate in all the cavity, this effect could be also seen for  $Re = 1000$  if the flow were computed at

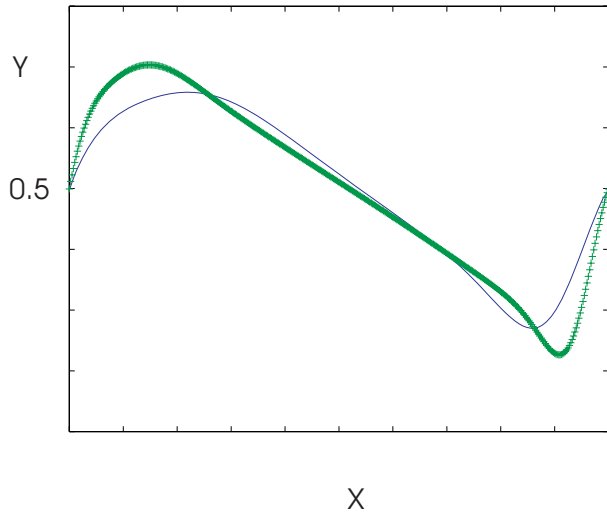


Figure 1: Profiles of  $u_2$  at  $y=0.5$ :  $Re=400$ ,  $h=1/100$  (-);  $Re=1000$ ,  $h=1/140$  (+)

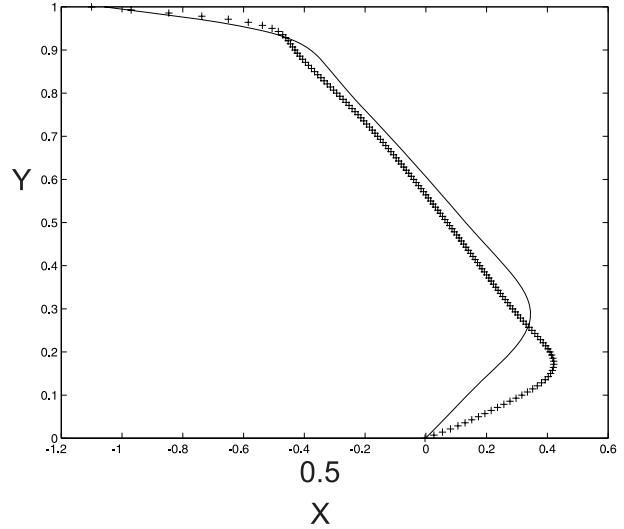


Figure 2: Profiles of  $u_1$  at  $x=0.5$ :  $Re=400$ ,  $h=1/100$  (-);  $Re=1000$ ,  $h=1/140$  (+)

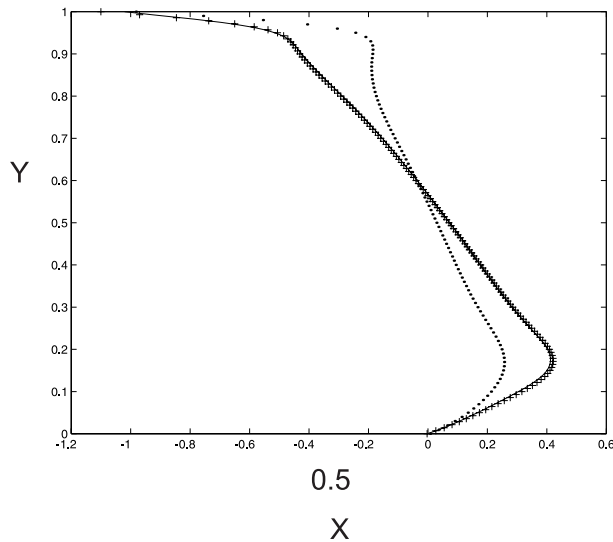


Figure 3:  $Re=1000$ ; profiles of  $u_1$  at  $x=0.5$ :  $h=1/400$  (-),  $h=1/140$  (+),  $h=1/100$  (...)

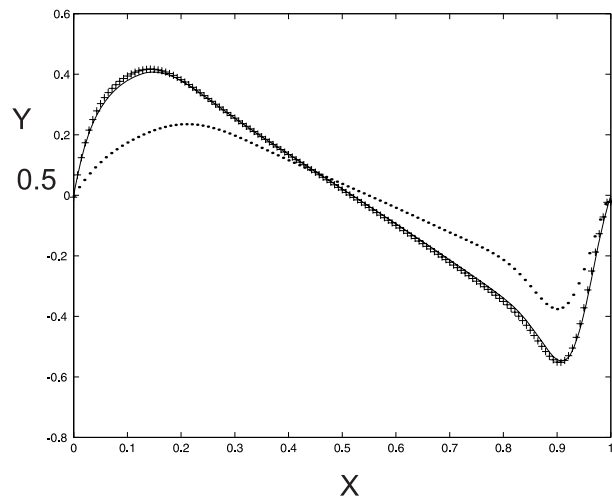


Figure 4:  $Re=1000$ ; profiles of  $u_2$  at  $y=0.5$ :  $h=1/400$  (-),  $h=1/140$  (+),  $h=1/100$  (...)

some  $T < 25$ ; the concentration being more and more in all the cavity for bigger Reynolds number (smaller viscosities), because the fluid motion is faster, as can be seen in Figures 8, 9, and 10. This phenomenon can be seen better looking backwards Figures 10, 9, 8, and 6, reminding that the vorticity contours are at the left of each picture. This vorticity "behavior" shows that the size of the meshes in addition to be demanded by the numerical procedure it reflects the physical meaning of the flow; of course, the finer the mesh for

higher  $Re$  the smaller the time step because of stability.

### 5 Conclusions

Numerical solutions of 2D viscous incompressible flows up to Reynolds numbers  $Re = 10000$  have been presented from the unsteady Navier-Stokes equations in velocity-vorticity formulation. These flows are obtained with a simple numerical procedure based mainly on a fixed point iterative process to solve the nonlinear elliptic

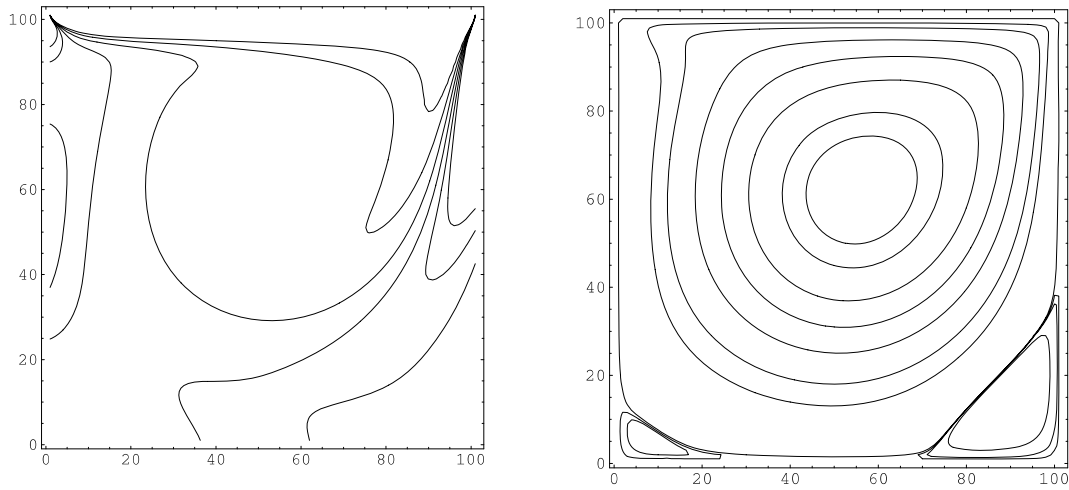


Figure 5:  $Re=400$  (vs S. & Keller)

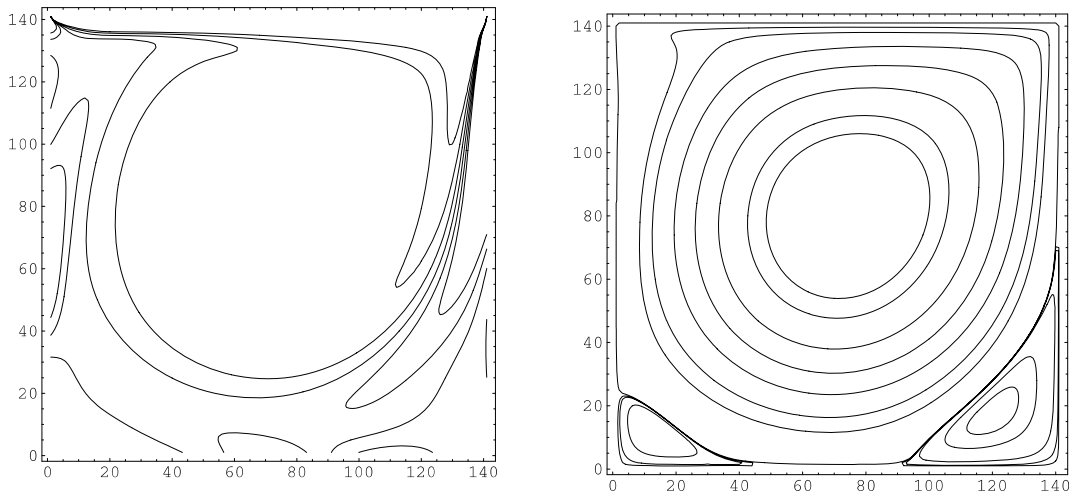


Figure 6:  $Re=1000$  (vs S. & Keller)

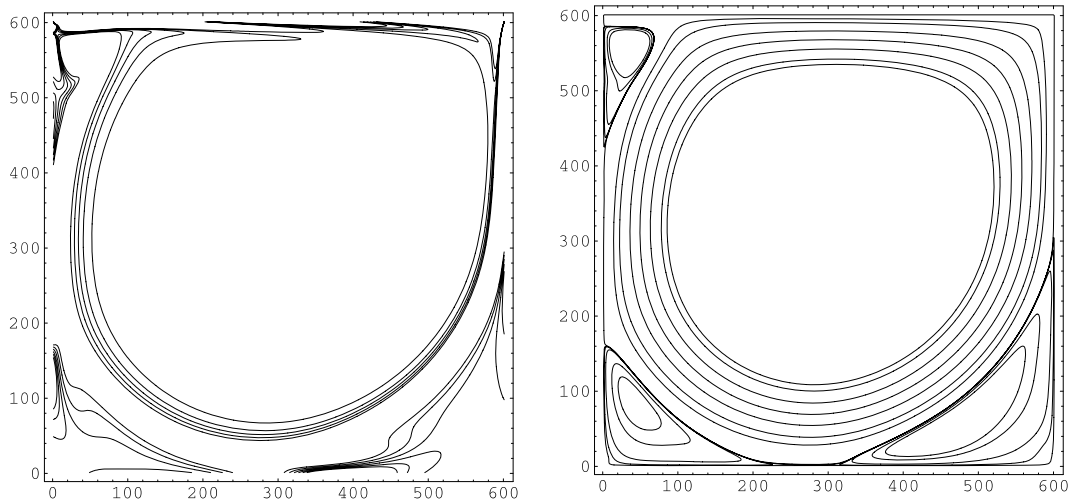


Figure 7:  $Re=4000$  (vs S. & Keller)

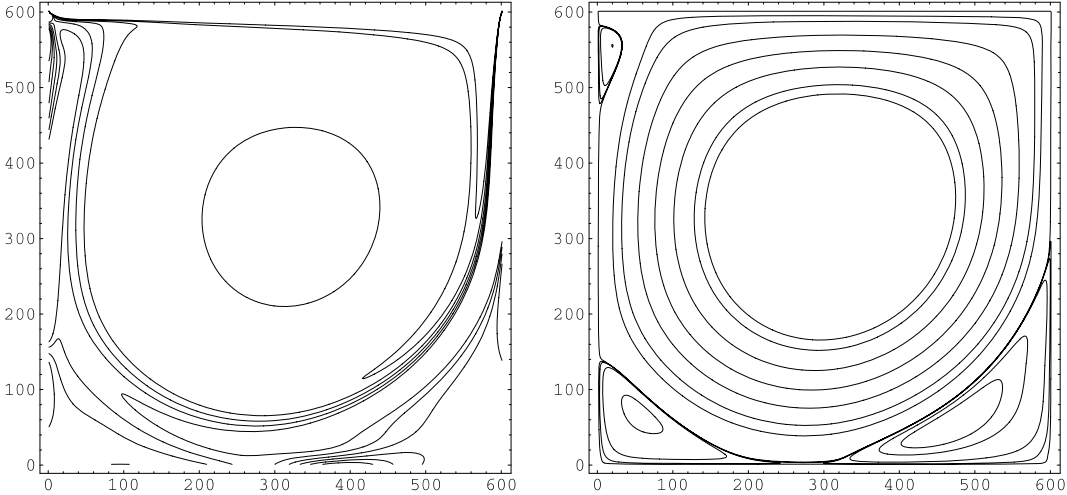


Figure 8:  $Re=4000$  at  $T=25$

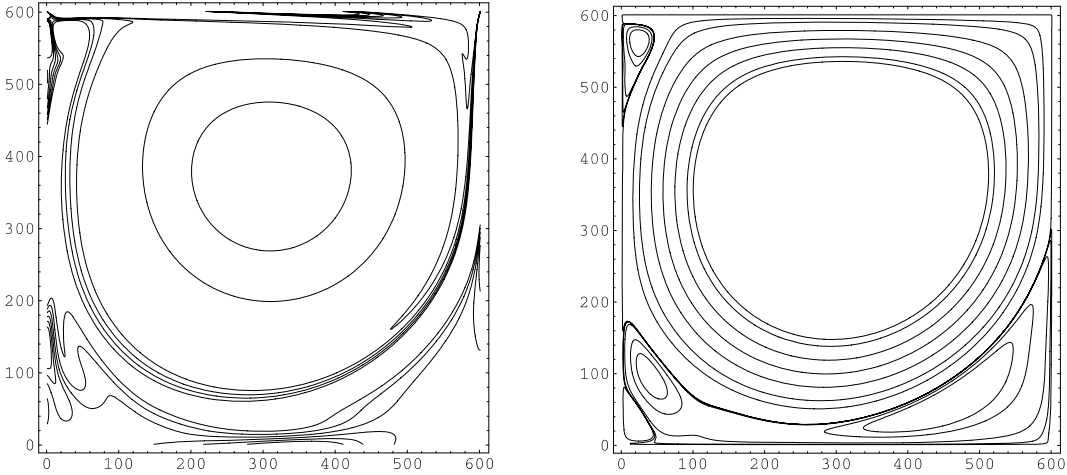


Figure 9:  $Re=5000$  at  $T=25$

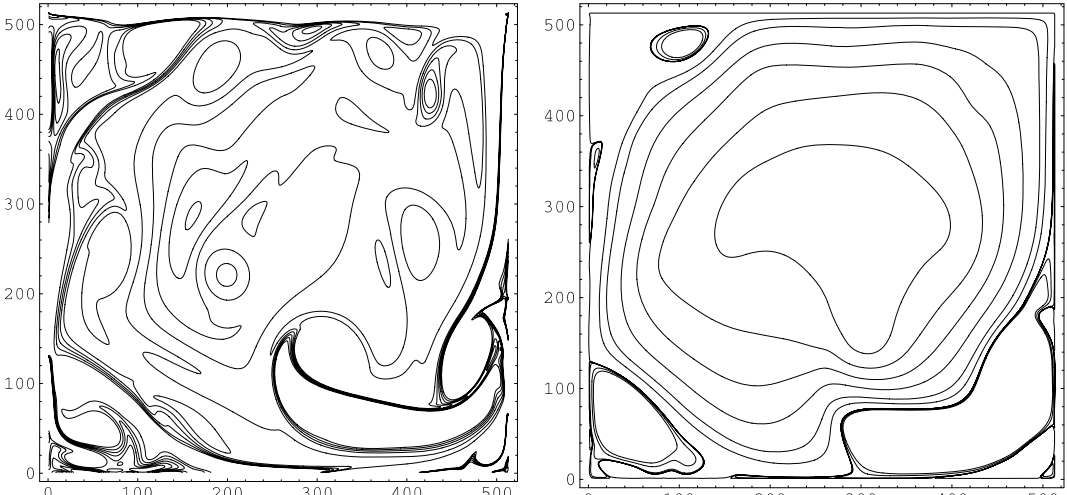


Figure 10:  $Re=10000$  at  $T=25$

system that results after an appropriate time discretization is made. The numerical procedure shows to be good capturing asymptotic steady states and computational experiments carried out so far indicate that it seems to be also able to computing flows for Reynolds numbers sufficiently large, close from its departure  $t = 0$ , to see how the flows look like. Even though that the numerical procedure applied to this formulation is not as good as the one applied to the stream function-vorticity formulation, the way it behaves, through the discretization parameters and even through the order of the discretization, gives us another point of view of the behavior of the flows under different numerical methods and different formulations of the problem, teaching us once again the difficulties associated with the numerical solution of the Navier-Stokes equations. On this regard, it is worth to mention that the difficulty with the vorticity-velocity formulation of the Navier-Stokes equations is reinforced through the works of Grimaldi et al. (2006) and Chantasiriwan (2006), mentioned in the Introduction, who with very different methods report driven cavity flows for Reynolds numbers not greater than ours; noticeable also is how similar the flow, for  $Re = 3200$  in Mai-Duy et al. (2007) from the stream function-vorticity formulation, looks like with ours at the final time  $T = 25$  for  $Re = 4000$ , concerning the vorticity iso-contours, showing the congruence of the different formulations. Moreover, the way the numerical method behaves for 2D flows gives bases to figure it out how close the method can handle the 3D formulation of velocity-vorticity formulation of the Navier-Stokes equations, or what kind of modifications must be done.

## References

**Adams J., Swarztrauber P. and Sweet R.** (1980): FISHPACK: A Package of Fortran Subprograms for the Solution of Separable Elliptic PDE's, *The National Center for Atmospheric Research*, Boulder, Colorado, USA.

**Bermúdez Blanca and Nicolás Alfredo** (1999): An Operator Splitting Numerical Scheme for Thermal/Isothermal Incompressible Viscous

Flows. *Int. J. Num. Meth. Fluids*, 29, 397-410.

**Burden R. L. and Faires J. D.** (1985): Numerical Analysis. PWS, Boston, USA.

**Fusegi T. and Farouk B.** (1986): Predictions of Fluid Flow and Heat Transfer Problems by the Vorticity-Velocity Formulation of the Navier-Stokes Equations. *J. Comp. Phys.* 65, 227-243.

**Ghia U., Ghia K.N., Shin C.T.** (1982): High-Re solutions for incompressible flow using the Navier-Stokes equations and a multigrid method. *J. Comp. Phys.* 48, 387-411.

**Glowinski R.** (2003): Handbook of Numerical Analysis: Numerical Methods for Fluids (Part 3). North-Holland Ed.

**Goyon O.** (1996): High-Reynolds number solutions of Navier-Stokes equations using incremental unknowns. *Comp. Methods Appl. Mech. Engrg.*, 130, 319-335.

**Grimaldi A., Pascazio G., Napolitano M.** (2006): A Parallell Multi-block Method for the Unsteady Vorticity-velocity Equations. *CMES: Computer Modeling in Engineering & Sciences*, Vol. 14, No. 1, 45-56.

**Gunzburger M. D.** (1989): Finite Element Methods for Viscous Incompressible Flows: A guide to theory, practice, and algorithms. Academic Press.

**Landau L.D. and Lifshitz E.M.** (1989): Fluid Mechanics, second edition. Pergamon Press.

**Lo D. C., Murugesan K., Young D. L.** (2005): Numerical solution of three-dimensional velocity-vorticity Navier-Stokes equations by finite difference method. *Int. J. Num. Meth. Fluids*, 47, 1469-1487.

**Mai-Duy N. and Tran-Cong T.** (2004): Boundary Integral-Based Domain Decomposition Technique of Navier-Stokes Equations. *CMES: Computer Modeling in Engineering & Sciences*, Vol. 6, No. 1, 59-75.

**Mai-Duy N., Mai-Cao L., Tran-Cong T.** (2007): Computation of transient viscous flows using indirect radial basis function networks. *CMES: Computer Modeling in Engineering & Sciences*, Vol. 18, No. 1, 59-77.

**Nicolás A. and Bermúdez B.** (2004): 2D Incompressible viscous flows at moderate and high

Reynolds numbers. *CMES: Computer Modeling in Engineering & Sciences*, Vol. 6, No. 5, 441-451.

**Nicolás A. and Bermúdez B.** (2005): 2D thermal/isothermal incompressible viscous flows. *Int. J. Numer. Meth. Fluids*, Vol. 48 349-366.

**Schreiber R., Keller H.B.** (1983): Driven cavity flow by efficient numerical techniques. *J. Comp. Phys.* 40, 310-333.

**Shu C., Ding H., Yeo K.S.** (2005): Computation of Incompressible Navier-Stokes Equations by Local RBF-based Differential Quadrature Method. *CMES: Computer Modeling in Engineering & Sciences*, Vol. 7, No. 2, 195-205.

**Sweet, R.** (1977): A cyclic reduction algorithm for solving block tri-diagonal systems of arbitrary dimensions. *SIAM J. N. Ana.*, 14, 706.

**Tsai, C., Young, D.L., Cheng A.H.** (2002): Meshless BEM for Three-Dimensional Stokes Flows. *CMES: Computer Modeling in Engineering & Sciences*, Vol. 3, No. 1, 117-128.

